

## STRESS SINGULARITY IN TORSION PROBLEM FOR BONDED BARS

TOMOAKI TSUJI and NAOTAKE NODA

Department of Mechanical Engineering, Shizuoka University, Jyooohoku 3-5-1, Hamamatsu 432, Japan

and

TOSHIKAZU SHIBUYA and TAKASHI KOIZUMI

Tokyo Institute of Technology, Ookayama, Meguro-ku, Tokyo 152, Japan

(Received 7 July 1989; in revised form 5 May 1990)

**Abstract**—Torsion problems for bonded bars composed of two semi-infinite bars bonded to each other by an elastic adhesive layer are investigated. Stress analysis proceeds considering the stress singularity at the corners by making use of the series expansion technique, and the problem is reduced to infinite sets of systems of linear equations. We introduce the generalized stress intensity factor at the corner. Stress fields in the neighborhood of the corners are shown by using only this factor. The values of the generalized stress intensity factor are obtained for the various mechanical and geometrical properties of the semi-infinite bars and adhesive layer.

### INTRODUCTION

A shaft is often constructed from different bars bonded to each other by an adhesive layer. When such a shaft is subjected to torsion, extremely high stresses are induced at the corner in the bonded surfaces. In such a kind of problem, the mechanical behavior of the adhesive layer is approximated by that of a spring (Erdogan and Ratwani, 1971; Tsuji *et al.*, 1985). However, when the adhesive layer is treated elastically, the stress singularity occurs at the corner. The problems related to this kind of singularity have been considered by many investigators. At first, Williams (1952) obtained the order of the stress singularity at the corner in extension problems. Keer and Freeman (1970) investigated the torsion of a finite elastic cylindrical rod partially bonded to an elastic half-space by using integral transform and Dini series. The authors treated the torsion problem of the stepped bar (Tsuji *et al.*, 1982) by using a series expansion technique. Karasudhi *et al.* (1984) investigated the torsion problem of a bar partially embedded in a layered elastic half space, and obtained the stress singularity at the corner for the torsion problem by using the method proposed by Williams (1952).

In such problems with the stress singularity, the generalized stress intensity factor, which is similar to the stress intensity factor for the crack, can be introduced at the corner. The stress fields in the neighborhood of the corner can be represented by this factor. Only a few investigations have been done, though this factor is important in order to consider the distraction of an object with corners. Theocaris and Petrou (1987) obtained the order of the singularity and this kind of factor near corners of a regular polygonal hole by using the complex stress function. Groth (1988) calculated the generalized stress intensity factor at the interface corners in bonded joints by using the finite element method and used it for the prediction of failure in some single lap joints. In our previous paper (Tsuji *et al.*, 1982), we did not obtain this parameter. Moreover, it is important to consider the adhesive layer for the problem of the stepped bar.

Therefore, we intend to investigate the generalized stress intensity factor in a torsion problem for a bonded bar, which is composed of two semi-infinite bars bonded to each other by an elastic adhesive layer. The stress analysis can be performed using a similar method to the previous paper (Tsuji *et al.*, 1982). In the present analysis we use Jacobi polynomials instead of Chebyshev polynomials, and some integrals of the products of the Bessel functions can be obtained in closed form. The relationships between the generalized

stress intensity factor and mechanical and geometrical properties of the semi-infinite bars and the adhesive layer are obtained.

STRESS FUNCTION

We use here the cylindrical coordinates  $(r, \theta, z)$ . In the case of an axisymmetric torsional stress field, the displacements and the stresses can be expressed by using Boussinesq's stress function  $\lambda_3(r, z)$  as follows :

$$v_\theta = -\frac{\partial \lambda_3}{\partial r}, \quad \tau_{\theta z} = -\frac{\partial^2 \lambda_3}{\partial r \partial z}, \quad \frac{\tau_{r\theta}}{G} = -\frac{\partial^2 \lambda_3}{\partial r^2} + \frac{1}{r} \frac{\partial \lambda_3}{\partial r}$$

$$u_r = w_z = 0, \quad \sigma_r = \sigma_\theta = \sigma_z = \tau_{rz} = 0 \tag{1}$$

where  $G$  is the shear modulus and  $\lambda_3(r, z)$  is an axisymmetric harmonic function.

STRESS ANALYSIS

We consider bonded shafts as shown in Fig. 1. These bonded bars are analyzed by separating into the semi-infinite circular cylinder domains [1], [2] and the adhesive layer domain [3] as shown in Fig. 1, and introducing continuity conditions on the  $z = 0$  and  $z = h$  planes. In the following expression, superscripts 1, 2 and 3 respectively denote quantities corresponding to the semi-infinite bars [1], [2] and the adhesive layer [3]. Thus, the boundary conditions are denoted as :

$$\tau'_{\theta z}(r, z) = 0, \quad T = 2\pi \int_0^{r_i} r^2 \tau'_{\theta z}(r, z) dr \begin{cases} h \leq z < \infty, & i = 1 \\ 0 \geq z > -\infty, & i = 2 \\ 0 \leq z < h, & i = 3 \end{cases} \tag{2}$$

$$\tau_{\theta z}^1(r, h) = \begin{cases} \tau_{\theta z}^1(r, h) & (0 \leq r \leq r_1) \\ 0 & (r_1 < r \leq r_2) \end{cases} \tag{3}$$

$$\tau_{\theta z}^2(r, 0) = \begin{cases} \tau_{\theta z}^2(r, 0) & (0 \leq r \leq r_2) \\ 0 & (r_2 < r \leq r_3) \end{cases} \tag{4}$$

$$v_\theta^1(r, h) = v_\theta^3(r, h) \quad (0 \leq r \leq r_1) \tag{5}$$

$$v_\theta^2(r, 0) = v_\theta^3(r, 0) \quad (0 \leq r \leq r_2) \tag{6}$$

where

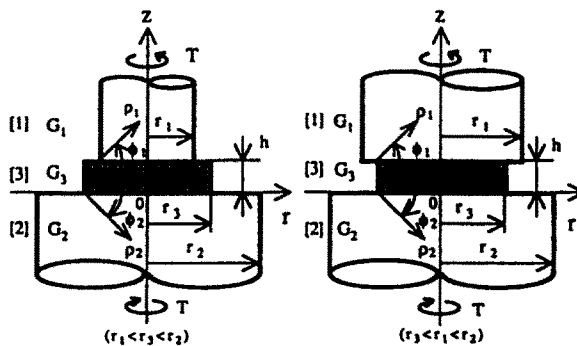


Fig. 1. Torsion problem of a bonded bar.

$$\begin{aligned} \xi = 1, \quad \eta = 3 \quad \text{when} \quad r_1 < r_3 < r_2 \\ \xi = 3, \quad \eta = 1 \quad \text{when} \quad r_3 < r_1 < r_2. \end{aligned}$$

In the following analysis, we use the subscripts  $\xi$  and  $\eta$  to represent the two cases  $r_1 < r_3 < r_2$  and  $r_3 < r_1 < r_2$ , respectively.

In the previous paper (Tsuji *et al.*, 1982), we represent the shear stress  $\tau_{\theta z}$  on the interface plane by using the Chebyshev polynomial in consideration of the stress singularity at the corner. However, in the present analysis, we should represent the shear stress  $\tau_{\theta z}$  on the  $z = 0$  and  $z = h$  planes by using the Jacobi polynomial  $G_n(p, q; x)$ , because the Jacobi polynomial has an orthogonal relationship with the weight function  $(1-x)^p x^q$  and some integrals of products of the Bessel functions and the Jacobi polynomials can be given in closed form. Hence, the shear stress  $\tau_{\theta z}$  on the  $z = 0$  and  $z = h$  planes are represented with respect to unknown coefficients  $x_k^i$  as follows:

$$\frac{\tau_{\theta z}^3(r, h)}{\tau^*} = \frac{\tau_{\theta z}^1(r, h)}{\tau^*} = \frac{r}{r_2} \left\{ 1 - \left( \frac{r}{r_2} \right)^2 \right\}^{-\kappa_1} \sum_{k=0}^{\infty} x_k^1 \frac{(-1)^k (1+k)! \Gamma(1-\kappa_1)}{\Gamma(1-\kappa_1+k)} G_k \left( 2-\kappa_1, 2; \frac{r^2}{r_2^2} \right) \quad (0 \leq r \leq r_2)$$

$$\frac{\tau_{\theta z}^2(r, 0)}{\tau^*} = \frac{\tau_{\theta z}^3(r, 0)}{\tau^*} = \frac{r}{r_3} \left\{ 1 - \left( \frac{r}{r_3} \right)^2 \right\}^{-\kappa_2} \sum_{k=0}^{\infty} x_k^2 \frac{(-1)^k (1+k)! \Gamma(1-\kappa_2)}{\Gamma(1-\kappa_2+k)} G_k \left( 2-\kappa_2, 2; \frac{r^2}{r_3^2} \right) \quad (0 \leq r \leq r_3) \quad (7)$$

where  $\kappa_i$  ( $i = 1, 2$ ) is the order of the stress singularity,  $\Gamma(x)$  is the Gamma function and  $\tau^*$  is the maximum shear stress when the bar [1] is subjected to the simple torque  $T$ :

$$\tau^* = 2T/(\pi r_1^3).$$

From eqns (2), (3) and (4),  $x_0^1, x_0^2$  can be obtained as:

$$x_0^1 = \frac{r_1^3}{r_2^3} \frac{(1-\kappa_1)(2-\kappa_1)}{2}, \quad x_0^2 = \frac{r_1^3}{r_3^3} \frac{(1-\kappa_2)(2-\kappa_2)}{2}. \quad (8)$$

To represent the stress fields with the unknown coefficients  $x_k^i$  ( $i = 1, 2$ ), we choose the stress function  $\lambda_j$  in the regions [1], [2] and [3], respectively, as follows:

$$\begin{aligned} \lambda_1^1(r, z) &= A'_0(r^2 - 2z^2) + A_0(2z^3 - 3r^2z) + \sum_{m=1}^{\infty} A_m J_0(\alpha_m r) e^{-\alpha_m(z-h)} \\ \lambda_2^2(r, z) &= B'_0(r^2 - 2z^2) + B_0(2z^3 - 3r^2z) + \sum_{m=1}^{\infty} B_m J_0(\beta_m r) e^{\beta_m z} \\ \lambda_3^3(r, z) &= C'_0(r^2 - 2z^2) + C_0(2z^3 - 3r^2z) + \sum_{m=1}^{\infty} [C_m^1 \cosh(\gamma_m z) + C_m^2 \cosh\{\gamma_m(z-h)\}] J_0(\gamma_m r) \end{aligned} \quad (9)$$

where  $J_n(x)$  is the first kind of Bessel function of order  $n$  and  $A_0, A'_0, A_m, \alpha_m$ , etc. are unknown coefficients which will be determined by the boundary conditions (2)–(6). Substituting these functions into eqn (1), displacement and stresses are given for each region. Using the boundary conditions (2),  $\alpha_m, \beta_m$  and  $\gamma_m$  are obtained as the positive roots of the following equation:

$$J_2(\alpha_m r_1) = 0, \quad \alpha_m r_1 = \beta_m r_2 = \gamma_m r_3 \quad (0 < \alpha_1 < \alpha_2 \dots). \quad (10)$$

Using the orthogonal relationship for the Bessel functions and the boundary conditions (3) and (4),  $A_0$ ,  $B_0$ ,  $C_0$ ,  $A_m$ ,  $B_m$  and  $C_m$  can be represented by  $x_k^1$  in eqn (7) as follows:

$$\begin{aligned} 6A_0 r_1 \frac{G_1}{\tau^*} &= \frac{r_1^3}{r_1^3} \frac{2}{(2-\kappa_1)(1-\kappa_1)} x_0^1 \\ 6B_0 r_2 \frac{G_2}{\tau^*} &= \frac{r_2^3}{r_2^3} \frac{2}{(2-\kappa_2)(1-\kappa_2)} x_0^2 \\ 6C_0 r_3 \frac{G_3}{\tau^*} &= \frac{r_3^3}{r_3^3} \frac{2}{(2-\kappa_1)(1-\kappa_1)} x_0^1 \\ &- A_m \alpha_m^2 \frac{G_1}{\tau^*} = \sum_{k=0}^{\infty} x_k^1 J_{k,m}^1 \left( \frac{r_2}{r_1} \right) \\ C_m^1 \gamma_m^2 \frac{G_3}{\tau^*} \sinh(\gamma_m h) &= \sum_{k=0}^{\infty} x_k^1 J_{k,m}^1 \left( \frac{r_2}{r_3} \right) \\ - C_m^2 \gamma_m^2 \frac{G_2}{\tau^*} \sinh(\gamma_m h) &= \sum_{k=0}^{\infty} x_k^2 J_{k,m}^2(1) \\ B_m \beta_m^2 \frac{G_2}{\tau^*} &= \sum_{k=0}^{\infty} x_k^2 J_{k,m}^2 \left( \frac{r_1}{r_2} \right) \end{aligned} \quad (11)$$

where  $J_{k,m}^i(t)$  is the integral of the product of the Bessel function and the Jacobi polynomial, and can be obtained in closed form as follows:

$$\begin{aligned} J_{k,m}^i(t) &= \frac{2(-1)^k (1+k)! \Gamma(1-\kappa_i) t^2}{\Gamma(1-\kappa_i+k) J_1^2(\alpha_m r_1)} \int_0^1 x^2 (1-x^2)^{-\kappa_i} G_k(2-\kappa_i, 2; x^2) J_1(t\alpha_m r_1 x) dx \\ &= (-1)^k G(1-\kappa_i) t^2 \left( \frac{t\alpha_m r_1}{2} \right)^{\kappa_i-1} \frac{J_{2-\kappa_i+2k}(t\alpha_m r_1)}{J_1^2(\alpha_m r_1)}. \end{aligned} \quad (12)$$

Substituting eqn (11) into eqns (9) and using eqn (1), the displacement and the stresses for each region are represented by  $x_k^i$  as:

[1] ( $h \leq z < \infty$ )

$$\begin{aligned} \frac{v_0^1 G_1}{r_1 \tau^*} &= -2A_0' \frac{r G_1}{r_1 \tau^*} + \frac{r z}{r_1^2} - \sum_{k=0}^{\infty} x_k^1 \sum_{m=1}^{\infty} \frac{J_{k,m}^1 \left( \frac{r_2}{r_1} \right)}{\alpha_m r_1} J_1(\alpha_m r) e^{-\alpha_m(z-h)} \\ \frac{\tau_{r\theta}^1}{\tau^*} &= \sum_{k=0}^{\infty} x_k^1 \sum_{m=1}^{\infty} J_{k,m}^1 \left( \frac{r_2}{r_1} \right) J_2(\alpha_m r) e^{-\alpha_m(z-h)} \\ \frac{\tau_{\theta z}^1}{\tau^*} &= \frac{r}{r_1} \sum_{k=0}^{\infty} x_k^1 \sum_{m=1}^{\infty} J_{k,m}^1 \left( \frac{r_2}{r_1} \right) J_1(\alpha_m r) e^{-\alpha_m(z-h)} \end{aligned} \quad (13)$$

[2]  $(-\infty < z \leq 0)$

$$\begin{aligned} \frac{v_0^3 G_1}{r_1 \tau^*} &= -2B_0' \frac{r G_1}{r_1 \tau^*} + \frac{G_1 r_1^4 r z}{G_2 r_2^4 r_1^2} + \frac{G_1}{G_2} \sum_{k=0}^{\infty} x_k^2 \sum_{m=1}^{\infty} \frac{J_{k,m}^2\left(\frac{r_3}{r_2}\right)}{\beta_m r_1} J_1(\beta_m r) e^{\beta_m z} \\ \frac{\tau_{\theta\theta}^2}{\tau^*} &= \sum_{k=0}^{\infty} x_k^2 \sum_{m=1}^{\infty} J_{k,m}^2\left(\frac{r_3}{r_2}\right) J_2(\beta_m r) e^{\beta_m z} \\ \frac{\tau_{\theta z}^2}{\tau^*} &= \frac{r_1^4 r}{r_2^4 r_1} + \sum_{k=0}^{\infty} x_k^2 \sum_{m=1}^{\infty} J_{k,m}^2\left(\frac{r_3}{r_2}\right) J_1(\beta_m r) e^{\beta_m z} \end{aligned} \tag{14}$$

[3]  $(0 \leq z \leq h)$

$$\begin{aligned} \frac{v_0^3 G_1}{r_1 \tau^*} &= -2C_0' \frac{r G_1}{r_1 \tau^*} + \frac{G_1 r_1^4 r z}{G_3 r_3^4 r_1^2} + \frac{G_1}{G_3} \sum_{k=0}^{\infty} x_k^1 \sum_{m=1}^{\infty} \frac{J_{k,m}^1\left(\frac{r_2}{r_3}\right) \cosh(\gamma_m z)}{\gamma_m r_1 \sinh(\gamma_m h)} J_1(\gamma_m r) \\ &\quad - \frac{G_1}{G_3} \sum_{k=0}^{\infty} x_k^2 \sum_{m=1}^{\infty} \frac{J_{k,m}^2(1) \cosh\{\gamma_m(z-h)\}}{\gamma_m r_1 \sinh(\gamma_m h)} J_1(\gamma_m r) \\ \frac{\tau_{\theta\theta}^3}{\tau^*} &= - \sum_{k=0}^{\infty} x_k^1 \sum_{m=1}^{\infty} J_{k,m}^1\left(\frac{r_2}{r_3}\right) \frac{\cosh(\gamma_m z)}{\sinh(\gamma_m h)} J_2(\gamma_m r) + \sum_{k=0}^{\infty} x_k^2 \sum_{m=1}^{\infty} J_{k,m}^2(1) \frac{\cosh\{\gamma_m(z-h)\}}{\sinh(\gamma_m h)} J_2(\gamma_m r) \\ \frac{\tau_{\theta z}^3}{\tau^*} &= \frac{r_1^4 r}{r_3^4 r_1} + \sum_{k=0}^{\infty} x_k^1 \sum_{m=1}^{\infty} J_{k,m}^1\left(\frac{r_2}{r_3}\right) \frac{\sinh(\gamma_m z)}{\sinh(\gamma_m h)} J_1(\gamma_m r) \\ &\quad - \sum_{k=0}^{\infty} x_k^2 \sum_{m=1}^{\infty} J_{k,m}^2(1) \frac{\sinh\{\gamma_m(z-h)\}}{\sinh(\gamma_m h)} J_1(\gamma_m r). \end{aligned} \tag{15}$$

Using the remaining boundary conditions (5) and (6), the equations with the unknown coefficients  $\{x_k^i\}$  are given as:

$$\begin{aligned} -2 \frac{r G_1}{r_1 \tau^*} (A_0' - C_0') + \left(1 - \frac{G_1 r_1^4}{G_3 r_3^4}\right) \frac{r h}{r_1^2} - \sum_{k=0}^{\infty} x_k^1 \sum_{m=1}^{\infty} \frac{J_{k,m}^1\left(\frac{r_2}{r_3}\right)}{\alpha_m r_1} J_1(\alpha_m r) \\ = \frac{G_1}{G_3} \sum_{k=0}^{\infty} x_k^1 \sum_{m=1}^{\infty} \frac{J_{k,m}^1\left(\frac{r_2}{r_3}\right) \cosh(\gamma_m h)}{\gamma_m r_1 \sinh(\gamma_m h)} J_1(\gamma_m r) \\ - \frac{G_1}{G_3} \sum_{k=0}^{\infty} x_k^2 \sum_{m=1}^{\infty} \frac{J_{k,m}^2(1)}{\gamma_m r_1 \sinh(\gamma_m h)} J_1(\gamma_m r) \quad (0 \leq r \leq r_2) \end{aligned} \tag{16}$$

$$\begin{aligned} -2 \frac{r G_1}{r_1 \tau^*} (C_0' - B_0') + \frac{G_1}{G_3} \sum_{k=0}^{\infty} x_k^1 \sum_{m=1}^{\infty} \frac{J_{k,m}^1\left(\frac{r_2}{r_3}\right)}{\gamma_m r_1 \sinh(\gamma_m h)} J_1(\gamma_m r) \\ - \frac{G_1}{G_3} \sum_{k=0}^{\infty} x_k^2 \sum_{m=1}^{\infty} \frac{J_{k,m}^2(1) \cosh(\gamma_m h)}{\gamma_m r_1 \sinh(\gamma_m h)} J_1(\gamma_m r) \\ = \frac{G_1}{G_2} \sum_{k=0}^{\infty} x_k^2 \sum_{m=1}^{\infty} \frac{J_{k,m}^2\left(\frac{r_3}{r_2}\right)}{\beta_m r_1} J_1(\beta_m r) \quad (0 \leq r \leq r_3). \end{aligned} \tag{17}$$

Equations (16) and (17) have the singularities  $(r_2 - r)^{1-\kappa_1}$  and  $(r_3 - r)^{1-\kappa_2}$  respectively. Thus, by considering these singularities, we multiply

$$\frac{r^2}{r_2^3} \left(1 - \frac{r^2}{r_2^2}\right)^{1-\kappa_1} G_n \left(3 - \kappa_1, 2; \frac{r^2}{r_2^2}\right)$$

and

$$\frac{r^2}{r_3^3} \left(1 - \frac{r^2}{r_3^2}\right)^{1-\kappa_2} G_n \left(3 - \kappa_2, 2; \frac{r^2}{r_3^2}\right)$$

by eqns (16) and (17), and integrate  $r = 0$  to  $r_2$  and  $r = 0$  to  $r_3$ , respectively, where we use  $G_n(3 - \kappa_i, 2; r^2/r_i^2)$  instead of  $G_n(2 - \kappa_i, 2; r^2/r_i^2)$ , because the convergence of  $A_{n,k}^{i,j}$  is faster. The following sets of algebraic equations with respect to  $\{x_k^i\}$  are given:

$$\sum_{k=0}^{\infty} x_k^1 A_{n,k}^{1,1} + \sum_{k=0}^{\infty} x_k^2 A_{n,k}^{1,2} = - \left\{ \frac{(A'_0 - C'_0)G_1}{\tau^*} - \frac{h}{2r_1} \left(1 - \frac{G_1 r_1^4}{G_3 r_3^4}\right) \right\} \frac{r_2^2}{r_1^3} \frac{2^{\kappa_1}}{\Gamma(4 - \kappa_1)} \delta_{n,0} \quad (n = 0, 1, 2, \dots) \quad (18)$$

$$\sum_{k=0}^{\infty} x_k^1 A_{n,k}^{2,1} + \sum_{k=0}^{\infty} x_k^2 A_{n,k}^{2,2} = - \frac{(B'_0 - C'_0)G_1}{\Gamma(4 - \kappa_2)\tau^*} 2^{\kappa_2} \frac{G_3 r_3^2}{G_1 r_1^2} \delta_{n,0} \quad (n = 0, 1, 2, \dots) \quad (19)$$

where

$$A_{n,k}^{1,1} = \sum_{m=1}^{\infty} \left(\frac{r_2}{r_1} \alpha_m^*\right)^{-3+\kappa_1} J_{k,m}^1 \left(\frac{r_2}{r_1}\right) J_{3-\kappa_1+2n} \left(\frac{r_2}{r_1} \alpha_m^*\right) + \frac{G_1}{G_3} \sum_{m=1}^{\infty} \left(\frac{r_2}{r_3} \alpha_m^*\right)^{-3+\kappa_1} E_m^1 J_{k,m}^1 \left(\frac{r_2}{r_3}\right) J_{3-\kappa_1+2n} \left(\frac{r_2}{r_3} \alpha_m^*\right)$$

$$A_{n,k}^{1,2} = - \frac{G_1}{G_3} \sum_{m=1}^{\infty} \left(\frac{r_2}{r_3} \alpha_m^*\right)^{-3+\kappa_1} E_m^2 J_{k,m}^2(1) J_{3-\kappa_1+2n} \left(\frac{r_2}{r_3} \alpha_m^*\right)$$

$$A_{n,k}^{2,1} = \sum_{m=1}^{\infty} (\alpha_m^*)^{-3+\kappa_2} E_m^2 J_{k,m}^1 \left(\frac{r_2}{r_3}\right) J_{3-\kappa_2+2n}(\alpha_m^*)$$

$$A_{n,k}^{2,2} = - \sum_{m=1}^{\infty} (\alpha_m^*)^{-3+\kappa_2} E_m^1 J_{k,m}^2(1) J_{3-\kappa_2+2n}(\alpha_m^*) - \frac{G_3}{G_2} \sum_{m=1}^{\infty} \left(\frac{r_3}{r_2} \alpha_m^*\right)^{-3+\kappa_2} J_{k,m}^2 \left(\frac{r_3}{r_2}\right) J_{3-\kappa_2+2n} \left(\frac{r_3}{r_2} \alpha_m^*\right)$$

$$\alpha_m^* = \alpha_m r_1, \quad E_m^1 = \frac{\cosh(\gamma_m h)}{\sinh(\gamma_m h)}, \quad E_m^2 = \frac{1}{\sinh(\gamma_m h)}$$

Consequently, the present problem is reduced to eqns (18) and (19).

### STRESS SINGULARITY

We introduce the generalized stress intensity factor  $K_i$  at the corners. This factor is similar to the stress intensity factor for a crack and can be defined as:

$$K_i = \lim_{\rho_i \rightarrow 0} \rho_i^{\kappa_i} (\tau_{\theta z}^i)_{\phi_i=0} \quad (i = 1, 2) \tag{20}$$

where  $(\rho_i, \phi_i)$  denotes polar coordinates as shown in Fig. 1. By substitution of eqn (7) into eqn (20),  $K_i$  is obtained with  $\{x_k^i\}$  as follows:

$$\frac{K_i}{\tau^* r_1^{\kappa_i}} = \begin{cases} 2^{-\kappa_1} \left(\frac{r_2}{r_1}\right)^{\kappa_1} \sum_{k=0}^{\infty} x_k^1 & (i = 1) \\ 2^{-\kappa_2} \left(\frac{r_3}{r_1}\right)^{\kappa_2} \sum_{k=0}^{\infty} x_k^2 & (i = 2). \end{cases} \tag{21}$$

In the neighborhood of the corners, in order to represent the shear stresses  $\tau_{r\theta}$  and  $\tau_{\theta z}$  in separating the singular terms, we expand  $J'_{k,m}(t) J_n(a\alpha_m r_1)$  by the first terms of the asymptotic expansion as follows for large  $m$ :

$$J'_{k,m}(t) J_n(a\alpha_m r_1) \approx -\Gamma(1-\kappa_i) 2^{-\kappa_i+1} a^{-1/2} t^{\kappa_i-1/2} (\alpha_m r_1)^{\kappa_i-1} \times \cos\left(t\alpha_m r_1 - \frac{1-2\kappa_i}{4}\pi\right) \cos\left(a\alpha_m r_1 - \frac{1+2n}{4}\pi\right). \tag{22}$$

Substituting eqn (22) into eqns (13)–(15) and using the following formulae:

$$\begin{aligned} \lim_{a \rightarrow 1} \sum_{m=1}^{\infty} J'_{k,m}(1) J_n(a\alpha_m r_1) e^{-b\alpha_m r_1} &\approx \frac{2^{-\kappa_i}}{\cos(\kappa_i\pi/2)} \{b^2 + (1-a)^2\}^{-\kappa_i/2} \sin\left(\kappa_i \arctan \frac{1-a}{b} + \frac{n}{2}\pi\right) \\ \lim_{a \rightarrow t} \sum_{m=1}^{\infty} J'_{k,m}(t) J_n(a\alpha_m r_1) e^{-b\alpha_m r_1} &\approx \frac{-2^{-\kappa_i} t^{\kappa_i}}{\cos(\kappa_i\pi/2)} \{b^2 + (t-a)^2\}^{-\kappa_i/2} \cos\left(\kappa_i \arctan \frac{t-a}{b} + \frac{n+\kappa_i}{2}\pi\right) \quad (t < 1), \end{aligned} \tag{23}$$

shear stresses  $\tau_{r\theta}$  and  $\tau_{\theta z}$  can be written by separating the singular terms as follows:

[1] ( $h \leq z < \infty$ )

$$\begin{aligned} \frac{\tau_{r\theta}^i}{\tau^*} &= \begin{cases} \left\{ \frac{\sin\left\{\kappa_i\left(\frac{\pi}{2}\phi_i\right)\right\}}{\cos(\pi\kappa_i/2)} \right\} \frac{K_i}{\tau^* r_1^{\kappa_i}} \left(\frac{\rho_i}{r_1}\right)^{-\kappa_i} & \text{when } r_1 < r_3 < r_2 \\ \left\{ -\frac{\cos\{\kappa_i(\pi-\phi_i)\}}{\cos(\pi\kappa_i)} \right\} \frac{K_i}{\tau^* r_1^{\kappa_i}} \left(\frac{\rho_i}{r_1}\right)^{-\kappa_i} & \text{when } r_3 < r_1 < r_2 \end{cases} \\ \frac{\tau_{\theta z}^i}{\tau^*} &= \begin{cases} \left\{ \frac{\cos\left\{\kappa_i\left(\frac{\pi}{2}-\phi_i\right)\right\}}{\cos(\pi\kappa_i/2)} \right\} \frac{K_i}{\tau^* r_1^{\kappa_i}} \left(\frac{\rho_i}{r_1}\right)^{-\kappa_i} & \text{when } r_1 < r_3 < r_2 \\ \left\{ \frac{\sin\{\kappa_i(\pi-\phi_i)\}}{\cos(\pi\kappa_i)} \right\} \frac{K_i}{\tau^* r_1^{\kappa_i}} \left(\frac{\rho_i}{r_1}\right)^{-\kappa_i} & \text{when } r_3 < r_1 < r_2 \end{cases} \end{aligned} \tag{24}$$

[2]  $(-\infty < z \leq 0)$ 

$$\begin{aligned}\frac{\tau_{r\theta}^2}{\tau^*} &= -\frac{\cos\{\kappa_2(\pi - \phi_2)\}}{\cos(\pi\kappa_2)} \frac{K_2}{\tau^* r_1^{\kappa_2}} \left(\frac{\rho_2}{r_1}\right)^{-\kappa_2} \\ \frac{\tau_{\theta z}^2}{\tau^*} &= \frac{\sin\{\kappa_2(\pi - \phi_2)\}}{\sin(\pi\kappa_2)} \frac{K_2}{\tau^* r_1^{\kappa_2}} \left(\frac{\rho_2}{r_1}\right)^{-\kappa_2}\end{aligned}\quad (25)$$

[3]  $(0 \leq z \leq h)$ 

$$\begin{aligned}\frac{\tau_{r\theta}^3}{\tau^*} &= \begin{cases} -\frac{\cos\{\kappa_1(\pi - \phi_1)\}}{\cos(\pi\kappa_1)} \\ \sin\left\{\kappa_1\left(\frac{\pi}{2} + \phi_1\right)\right\} \\ -\frac{\cos(\pi\kappa_1/2)}{\cos(\pi\kappa_1/2)} \end{cases} \frac{K_1}{\tau^* r_1^{\kappa_1}} \left(\frac{\rho_1}{r_1}\right)^{-\kappa_1} & \text{when } r_1 < r_3 < r_2 \\ & \frac{K_1}{\tau^* r_1^{\kappa_1}} \left(\frac{\rho_1}{r_1}\right)^{-\kappa_1} & \text{when } r_3 < r_1 < r_2 \\ & -\frac{\sin\left\{\kappa_2\left(\frac{\pi}{2} + \phi_2\right)\right\}}{\cos(\pi\kappa_2/2)} \frac{K_2}{\tau^* r_1^{\kappa_2}} \left(\frac{\rho_2}{r_1}\right)^{-\kappa_2} \\ \frac{\tau_{\theta z}^3}{\tau^*} &= \begin{cases} \frac{\sin\{\kappa_1(\pi - \phi_1)\}}{\sin(\pi\kappa_1)} \\ \cos\left\{\kappa_1\left(\frac{\pi}{2} + \phi_1\right)\right\} \\ \frac{\cos(\pi\kappa_1/2)}{\cos(\pi\kappa_1/2)} \end{cases} \frac{K_1}{\tau^* r_1^{\kappa_1}} \left(\frac{\rho_1}{r_1}\right)^{-\kappa_1} & \text{when } r_1 < r_3 < r_2 \\ & \frac{K_1}{\tau^* r_1^{\kappa_1}} \left(\frac{\rho_1}{r_1}\right)^{-\kappa_1} & \text{when } r_3 < r_1 < r_2 \\ & + \frac{\cos\left\{\kappa_2\left(\frac{\pi}{2} + \phi_2\right)\right\}}{\cos(\pi\kappa_2/2)} \frac{K_2}{\tau^* r_1^{\kappa_2}} \left(\frac{\rho_2}{r_1}\right)^{-\kappa_2}.\end{aligned}\quad (26)$$

Hence, the stress fields in the neighborhood of the corners are obtained by the generalized stress intensity factor  $K_i$ . By using the relationship between the shear stress  $\tau_{r\theta}$  and the displacement  $v_\theta$  as:

$$\frac{\tau_{r\theta}}{G} = r \frac{\partial}{\partial r} \left( \frac{v_\theta}{r} \right),$$

eqns (5) and (6) are rewritten as follows:

$$\begin{aligned}\frac{\tau_{r\theta}^1}{G_1} &= \frac{\tau_{r\theta}^3}{G_3} \quad (z = h, \phi_1 = 0, 0 \leq r \leq r_2) \\ \frac{\tau_{r\theta}^2}{G_2} &= \frac{\tau_{r\theta}^3}{G_3} \quad (z = 0, \phi_2 = 0, 0 \leq r \leq r_3).\end{aligned}\quad (27)$$

Substituting eqns (24)–(26) into eqn (27), the following equations with respect to the order of the singularity  $\kappa_i$  are obtained:

$$\cos(\pi\kappa_1) = \frac{1}{1 + \frac{G_2}{G_1}}, \quad \cos(\pi\kappa_2) = \frac{1}{1 + \frac{G_3}{G_2}}.\quad (28)$$



The order of the stress singularity  $\kappa$ , is related to the shear moduli  $G_i$  ( $i = 1, 2, 3$ ) only, and eqn (28) is the same as the one obtained by Keer and Freeman (1970) for a bar bonded to a half space and Karasudhi *et al.* (1984) by using Williams' method (1952).

NUMERICAL RESULTS

In order to obtain accurate values of the generalized stress intensity factor  $K_i$ , we should investigate the convergence of the infinite series in eqn (21) with respect to  $x_k^i$  and get accurate values of  $A_{n,k}^{i,j}$  in eqns (18) and (19) in order to get  $x_k^i$  accurately. In the previous paper, we could obtain the values of the coefficients as  $A_{n,k}^{i,j}$  by truncating the infinite series, because we did not calculate any value of the generalized stress intensity factor. But, in the present investigation, we must get accurate values of  $A_{n,k}^{i,j}$  to obtain the accurate generalized stress intensity factor. Thus, by using the asymptotic expansion as shown in the Appendix, we calculate the remaining values of  $A_{n,k}^{1,1}$  and  $A_{n,k}^{2,2}$  in closed form. These coefficients are exact in five-digits with 1000 terms. The values of  $A_{n,k}^{1,2}$  and  $A_{n,k}^{2,1}$  can be obtained very accurately by truncating at the number 200, because there are terms of  $1/\sinh(\gamma_m h)$  in these series. Consequently we can get accurate values of  $A_{n,k}^{i,j}$  with the compact numerical calculations. In Fig. 2, we show the relationship between the values of  $K_i$  (for  $r_2/r_1 = 2.0$ ,  $r_3/r_1 = 1.2$ ,  $G_2/G_1 = 1.0$ ,  $G_3/G_1 = 0.5$ ) and the reciprocal of truncated number  $L$  in the infinite series in eqn (21). With decreasing  $h$ , the convergence of  $K_2$  is slow, although, in this case, the error of  $K_2$  is not important, because the value of  $K_2$  is smaller than the one of  $K_1$  and decreases with decreasing  $h$ . Moreover, the case when  $h/r_1 < 0.05$  and  $r_3 < r_1$  is the one with the worst convergence of  $K_2$ . When  $r_3$  is bigger than  $r_1$ , both of the series for  $K_1$  and  $K_2$  converge as well as  $K_1$  in Fig. 2. From Fig. 2, it is shown that we can get

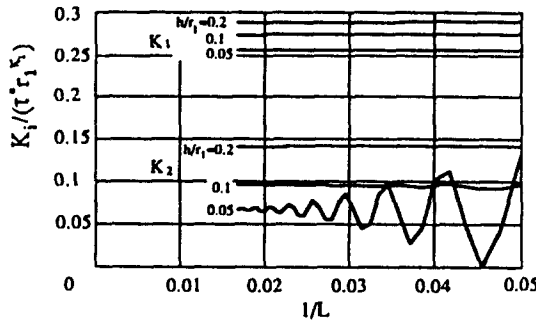


Fig. 2. The convergence of the generalized stress singularity  $K_i$ .

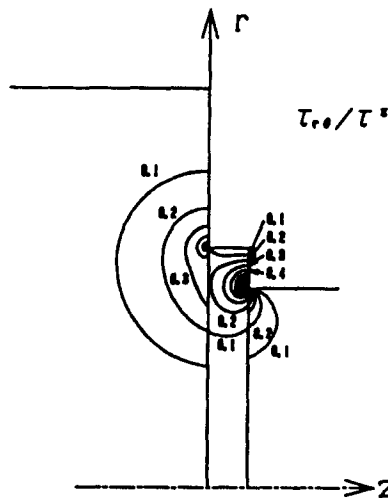


Fig. 3. Constant  $\tau_{\theta z}$  lines ( $h/r_1 = 0.2$ ,  $r_2/r_1 = 2.0$ ,  $r_3/r_1 = 1.2$ ,  $G_2/G_1 = 1.0$ ,  $G_3/G_1 = 0.5$ ).

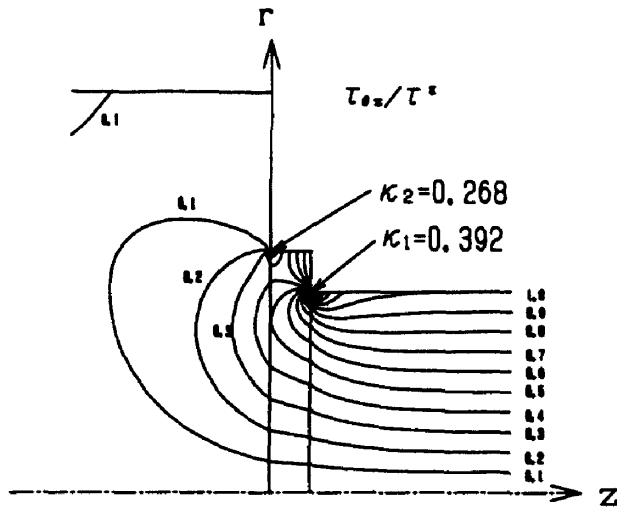


Fig. 4. Constant  $\tau_{\theta z}$  lines ( $h/r_1 = 0.2$ ,  $r_2/r_1 = 2.0$ ,  $r_3/r_1 = 1.2$ ,  $G_2/G_1 = 1.0$ ,  $G_3/G_1 = 0.5$ ).

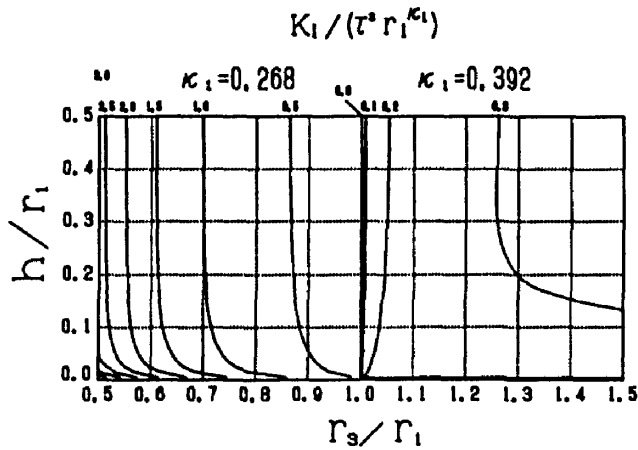


Fig. 5. Constant  $K_1$  lines ( $G_2/G_1 = 1.0$ ,  $G_3/G_1 = 0.5$ ,  $r_2/r_1 = 2.0$ ).

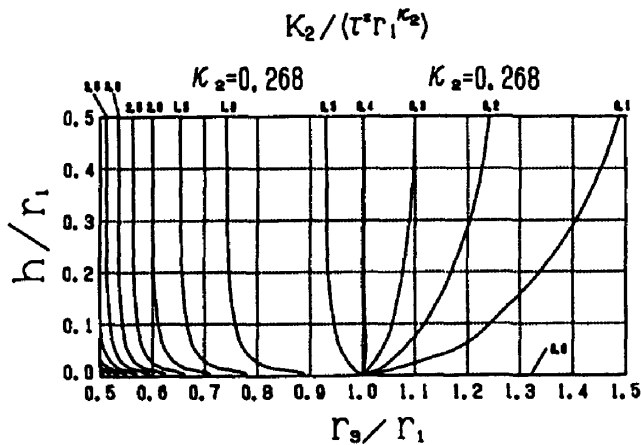


Fig. 6. Constant  $K_2$  lines ( $G_2/G_1 = 1.0$ ,  $G_3/G_1 = 0.5$ ,  $r_2/r_1 = 2.0$ ).

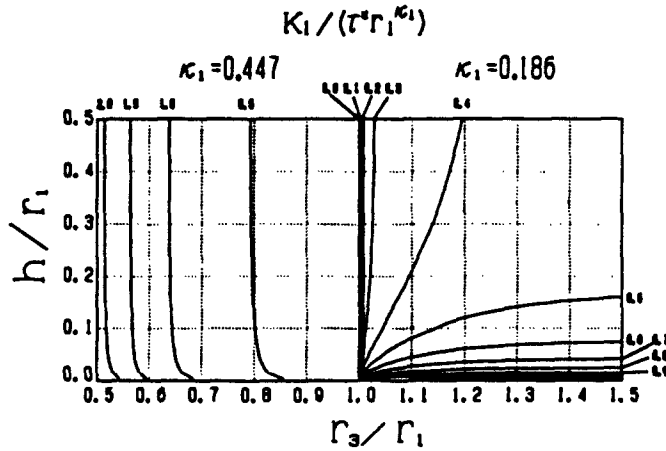


Fig. 7. Constant  $K_1$  lines ( $G_2/G_1 = 1.0, G_3/G_1 = 5, r_2/r_1 = 2.0$ ).

satisfactorily accurate values for  $K_i$  by truncating at the number  $L = 50$ . Accordingly, in the following calculations, we use the number  $L = 50$ .

Figures 3 and 4 show the constant stress lines of shear stresses  $\tau_{\theta z}$  and  $\tau_{r\theta}$  (for  $h/r_1 = 0.2, r_2/r_1 = 2.0, r_3/r_1 = 1.2, G_2/G_1 = 1.0, G_3/G_1 = 0.5$ ). Since the shear modulus is discontinuous at the  $z = 0$  and  $h$  planes,  $\tau_{r\theta}$  is discontinuous at these planes. Stresses are concentrated at the corners. The values of stresses in the neighborhood of  $z = h, r = r_1$  are bigger than the ones at  $z = 0, r = r_2$ .

In order to investigate the relationship between these stress concentrations and the geometry of the adhesive layer, we show the generalized stress intensity factor  $K_i$  denoted in eqn (20) in Figs 5-8. Figures 5 and 6 show the relationship between  $K_i, h$  and  $r_3$  with  $G_2/G_1 = 1.0, G_3/G_1 = 0.5$  and  $r_2/r_1 = 2.0$ . When  $r_3$  is smaller than  $r_1$  and  $h \rightarrow 0$ , the problem tends to the crack problem. Since the order of the stress singularity for the crack is  $1/2$  and this order is bigger than the one for the corner,  $K_i$  increases to infinity with decreasing  $h$ . In Fig. 5, when  $r_3$  is bigger than  $r_1, K_1$  decreases to zero with decreasing  $h$ , because the order of the singularity is  $1/3$  with  $h = 0$  and smaller than 0.392. In Fig. 6, when  $r_3$  is bigger than  $r_1, K_2$  decreases to zero with decreasing  $h$ , because this corner is a free surface with  $h = 0$ . Figures 7 and 8 show the relationship between  $K_i, h$  and  $r_1$  with  $G_3/G_1 = 5.0, G_2/G_1 = 1.0$  and  $r_2/r_1 = 2.0$ . In Fig. 7, when  $r_3$  is bigger than  $r_1, K_1$  increases to infinity with decreasing  $h$ , because the order of the singularity is  $1/3$  with  $h = 0$  and bigger than 0.186.

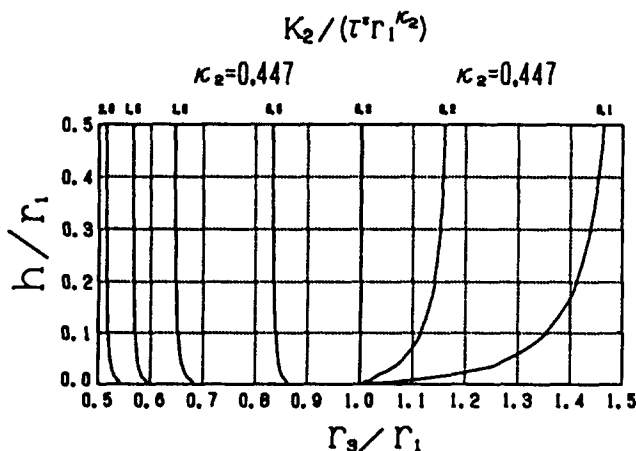


Fig. 8. Constant  $K_2$  lines ( $G_2/G_1 = 1.0, G_3/G_1 = 5, r_2/r_1 = 2.0$ ).

Table 1. The thickness of the adhesive layer which reduces  $K_1$ .

	$G_1 = G_2 < G_3$	$G_1 = G_2 > G_3$
$r_1 < r_3 < r_2$	X	Thinner
$r_3 < r_1 < r_2$	Thicker	Thicker

Table 1 shows the choices of the thickness of the adhesive layer  $h$  which make stress fields in the neighborhood of the corners smaller. When  $r_1 < r_3 < r_2$  and  $G_1 = G_2 < G_3$ , we cannot select the thickness of the adhesive layer, because there is a conflict in the behavior of  $K_1$  and  $K_2$  with respect to  $h$ . Therefore, we should choose the appropriate thickness by considering the values of  $K_1$  and  $K_2$ .

CONCLUSIONS

The generalized stress intensity factor at the corners of a bonded bar under torsion was obtained. The analysis was performed by making use of the series expansion technique with consideration of the stress singularity at the corners. The generalized stress intensity factor was introduced at the corners, and the stress fields in the neighborhood of the corners were shown by this factor. By these results, the stress singularities at each corner were obtained. By numerical calculation, values of the generalized stress intensity factor at the corners were obtained for the various mechanical and geometrical properties of the bars and the adhesive layer, and these results were shown graphically. From these figures, it was shown how to choose the thickness of the adhesive layer.

REFERENCES

Erdogan, F. and Ratwani, M. (1971). Stress distribution in bonded joints. *J. Compos. Mater.* **5**, 378.  
 Groth, H. L. (1988). Stress singularities and fracture at interface corners in bonded joints. *Int. J. Adhesion and Adhesives* **8**, 107.  
 Karasudhi, P., Rajapakse, R. K. N. D. and Hwang, B. (1984). Torsion of a long cylindrical elastic bar partially embedded in a layered elastic half space. *Int. J. Solids Structures* **20**, 1.  
 Keer, L. M. and Freeman, N. J. (1970). Load transfer problem for an embedded shaft in torsion. *Trans. ASME Ser. E* **92**, 959.  
 Theocaris, P. S. and Petrou, L. (1987). The order of singularities and the stress intensity factors near corners of regular polygonal holes. *Int. J. Engng Sci.* **25**, 821.  
 Tsuji, T., Shibuya, T. and Koizumi, T. (1982). The stress singularity in a stepped cylindrical rod under torsion. *Theor. Appl. Mech.* **31**, 63.  
 Tsuji, T., Shibuya, T., Koizumi, T. and Takakuda, K. (1985). Torsion problem for bonded rods. *Bull. JSME* **28**, 2547.  
 Williams, M. L. (1952). Stress singularities resulting from various boundary conditions in angular corners of plates in extension. *J. Appl. Mech. ASME* **19**, 526.

APPENDIX

Asymptotic expansion for large  $m$ :

$$(x_m^*) \sim \frac{J_a(sx_m^*)J_b(sx_m^*)}{J_c^2(x_m^*)} \approx \frac{1}{2} \sum_{i=0}^{\infty} \sum_{j=0}^{\infty} \{(i+j+m)\pi\}^{-i-j} \left[ \cos \left\{ \frac{a-b-\text{mod}(i/2)}{2} \pi \right\} \right. \\
 \left. + \cos \left\{ 2jm\pi + \frac{3s-a-b-1+2j-\text{mod}(i/2)}{2} \pi \right\} \right] C_i'(a, b, s, r) \quad (A1)$$

where

$$C_0^0(a, b, s, r) = 1, \quad C_0^1(a, b, s, r) = 0, \\
 C_1^0(a, b, s, r) = \frac{1}{8s} (15s^2 - 4b^2 + 1), \quad C_1^1(a, b, s, r) = C_1^0(b, a, s, r), \\
 C_2^0(a, b, s, r) = \frac{1}{64s^2} \{ -225s^4 + 2s^2(30a^2 + 30b^2 + 60r + 77) - 8(a^4 + b^4) + 20(a^2 + b^2) - 9 \}$$

$$C_2^1(a, b, s, r) = \frac{1}{64s^2} [225s^4 + 30s^2 \{-2(a^2 + b^2) + 1\} - 16(ab)^2 - 4(a^2 + b^2) + 1]$$

$$C_3^0(a, b, s, r) = \frac{1}{768s^3} [-3375s^6 + 135s^4 \{10(a^2 + b^2) + 20r + 33\} + 45s^2 \{-4(a^4 + b^4) - 4(2b^2 + 5 + 4r)a^2 + 12b^2 + 4r + 3\} + 16a^6 - 140a^4 + 2a^2(24b^4 - 60b^2 + 143) + 3(-4b^4 + 10b^2 - 21)]$$

$$C_3^1(a, b, s, r) = C_3^0(b, a, s, r) \dots$$

The summation of the right hand of eqn (A1) with  $m = M$  to infinity can be obtained in closed form by using the following formulae:

$$\sum_{m=M}^{\infty} (x+m)^{-r} = \zeta(r, x) - \sum_{m=1}^{M-1} (x+m)^{-r} \tag{A2}$$

$$\sum_{m=M}^{\infty} (x+m)^{-r} \cos(2sm\pi + x) = \sum_{k=K_0}^{K_0+M_1-1} M_1^{-r} \cos(2sk\pi + x) \left\{ \zeta\left(r, \frac{x+k}{M_1}\right) - \sum_{m=1}^{K_1-1} \left(\frac{x+k}{M_1} + m\right)^{-r} \right\} \tag{A3}$$

where  $M_1$ ,  $K_0$  and  $K_1$  are the integer values which are given by the following equations:

$$s = \frac{N_1}{M_1}, \quad K_0 = \text{mod}\left(\frac{M}{M_1}\right), \quad K_1 = \text{int}\left(\frac{M}{M_1}\right).$$

$\zeta(r, x)$  is the generalized zeta function defined as follows:

$$\zeta(r, x) = \sum_{k=1}^{\infty} (x+k)^{-r}.$$

Accordingly, summation of the left hand side of eqn (A1) can be obtained in closed form as follows:

$$\sum_{m=1}^l (x_m^*)^{-r} \frac{J_a(sx_m^*) J_b(sx_m^*)}{J_i^2(x_m^*)} \cong \sum_{m=1}^{M-1} (x_m^*)^{-r} \frac{J_a(sx_m^*) J_b(sx_m^*)}{J_i^2(x_m^*)} + \frac{1}{2} \sum_{i=0}^l \pi^{-r} \sum_{j=0}^1 \left[ \zeta\left(r+i, \frac{1}{2}\right) - \sum_{m=1}^{M-1} \left(\frac{1}{2} + m\right)^{-r} \right] \cos\left\{ \frac{a-b-\text{mod}(i/2)}{2} \pi \right\} + \sum_{k=K_0}^{K_0+M_1-1} M_1^{-r} \left\{ \zeta\left(r+i, \frac{1}{2} + \frac{k}{M_1}\right) - \sum_{m=1}^{K_1-1} \left(\frac{1}{2} + \frac{k}{M_1} + m\right)^{-r} \right\} \times \cos\left( 2sk\pi + \frac{3s-a-b-1+2j-\text{mod}(i/2)}{2} \pi \right) C_l^i(a, b, s, r+i). \tag{A4}$$

In Table A1, the values of eqn (A4) are listed for various values of  $a, b, s, r$  and  $M$  with  $l = 5$ .

Table A1. The convergence of infinite series.

a	b	s	r	M				Converged
				100	200	500	1000	
10	10	1.0	3.3	0.74031e-03	0.74031e-03	0.74031e-03	0.74031e-03	0.74031e-03
10	20	1.0	3.3	0.11418e-05	0.11418e-05	0.11418e-05	0.11418e-05	0.11418e-05
10	40	1.0	3.3	0.88299e-08	0.98284e-08	0.98293e-08	0.98293e-08	0.98293e-08
10	80	1.0	3.3	-0.71744e-05	-0.11054e-07	0.98300e-10	0.99429e-10	0.99430e-10
20	20	1.0	3.3	0.14913e-03	0.14913e-03	0.14913e-03	0.14913e-03	0.14913e-03
20	40	1.0	3.3	-0.40925e-07	-0.46724e-07	-0.46729e-07	-0.46729e-07	-0.46729e-07
20	80	1.0	3.3	0.30020e-04	0.46539e-07	-0.40886e-09	-0.41363e-09	-0.41363e-09
40	40	1.0	3.3	0.30462e-04	0.30231e-04	0.30230e-04	0.30230e-04	0.30230e-04
40	80	1.0	3.3	0.14968e-03	0.25193e-06	-0.18960e-08	-0.19232e-08	-0.19232e-08
80	80	1.0	3.3	0.30382e-02	0.13408e-04	0.61374e-05	0.61363e-05	0.61363e-05